Transitions in Early Embryonic Atrioventricular Valvular Function Correspond With Changes in Cushion Biomechanics That Are Predictable by Tissue Composition

Jonathan T. Butcher, Tim C. McQuinn, David Sedmera, Debi Turner and Roger R. Markwald

Circ. Res. 2007;100;1503-1511; originally published online May 3, 2007;
DOI: 10.1161/CIRCRESAHA.107.148684
Circulation Research is published by the American Heart Association. 7272 Greenville Avenue, Dallas, TX 72514
 Print ISSN: 0009-7330. Online ISSN: 1524-4571

Transitions in Early Embryonic Atrioventricular Valvular Function Correspond With Changes in Cushion Biomechanics That Are Predictable by Tissue Composition

Jonathan T. Butcher, Tim C. McQuinn, David Sedmera, Debi Turner, Roger R. Markwald

Abstract—Endocardial cushions are critical to maintain unidirectional blood flow under constantly increasing hemodynamic forces, but the interrelationship between endocardial cushion structure and the mechanics of atrioventricular junction function is poorly understood. Atrioventricular (AV) canal motions and blood velocities of embryonic chicks at Hamburger and Hamilton (HH) stages 17, 21, and 25 were quantified using ultrasonography. Similar to the embryonic zebrafish heart, the HH17 AV segment functions like a suction pump, with the cushions expanding in a wave during peak myocardial contraction and becoming undetectable during the relaxation phase. By HH25, the AV canal contributes almost nothing to the piston-like propulsion of blood, but the cushions function as stoppers apposing blood flow with near constant thickness. Using a custom built mesomechanical testing system, we quantified the nonlinear pseudoelastic biomechanics of developing AV cushions, and found that both AV cushions increased in effective modulus between HH17 and HH25. Enzymatic digestion of major structural constituent collagens or glycosaminoglycans resulted in distinctly different stress-strain curves suggestive of their individual contributions. Mixture theory using histologically determined volume fractions of cells, collagen, and glycosaminoglycans showed good prediction of cushion material properties regardless of stage and cushion position. These results have important implications in valvular development, as biomechanics may play a larger role in stimulating valvulogenic events than previously thought. (***Circ Res*. 2007;100:1503-1511.)**

Key Words: chick ■ development ■ modeling ■ ultrasound ■ flow ■ aspiration

The development of the atrioventricular (AV) and semilunar valves of the heart from the endocardial cushions occurs concomitantly with a constant barrage of hemodynamic and mechanical forces. Several studies have demonstrated that both blood pressure and velocities increase during morphological development in the heart, implying that the stresses on the endocardial cushions are also increasing.[1–3] Early investigations highlighted the motions of cushions in concert with the contracting myocardium, suggesting that they serve a valve-like function before valves form.[4] However, a recent study showed that the atrioventricular canal in the tubular early zebrafish heart functions like a suction pump, in contrast to the peristaltic mechanism previously described.[5] These observations raise no controversy with respect to current understanding of transitions that occur structurally and molecularly in the myocardium during early tube heart development, but raise major questions with respect to the mechanism through which endocardial cushions function in promoting unidirectional blood flow during the transition from tubular heart to a septated structure. In this study we examined the mechanical properties and myocardial/endocardial cushion mechanical interaction in 3 stages of cardiac development in the chick embryo to better understand how the mechanical properties of the cushions contribute to their functional roles.

Various mutant models demonstrate that genetic defects compromising valve structural maturation result in severe regurgitation, dilatation, and lethality, suggesting that the appropriate maturation of valve matrix is essential for continued function.[6,7] These models add weight to the argument that structural properties of AV cushion tissue may be critical determinants of AV cushion function, and that abnormal AV cushion tissue properties (other than mass, which has been well documented) may result in physiological abnormalities in blood flow and cardiac mechanical function before gross morphological disturbances are seen. A link between myocardial elastic and viscous material properties and structural development exists,[8,9] and changes in these properties from altered hemodynamic loading argue that mechanical forces do shape embryonic cardiac structural development.[1,9–11] The

Original received January 16, 2007; revision received March 14, 2007; accepted April 23, 2007.

From the Department of Cell Biology and Anatomy (J.T.B., T.C.M., D.S., D.T., R.R.M.) and the Department of Pediatrics (Cardiology) (J.T.B., T.C.M.), Cardiovascular Developmental Biology Center, Children's Research Institute, Medical University of South Carolina, Charleston; and the Institute of Animal Physiology and Genetics (D.S.), Videnska, and the Institute of Anatomy, 1st Faculty of Medicine (D.S.), Charles University, Prague, Czech Republic.

Correspondence to Jonathan T. Butcher, Department of Biomedical Engineering, 270 Olin Hall, Cornell University, Ithaca NY. Email jtb47@cornell.edu

Circulation Research **is available at http://circres.ahajournals.org** **DOI: 10.1161/CIRCRESAHA.107.148684**

relationship between mechanics and structure in adult valves[10–12] has been studied, but not in embryonic cushions. Therefore, connections between cushion structure, hemodynamics, and biomechanics may form a basis for quantifying normal and abnormal embryonic valve function. In this paper we have combined state of the art ultrasonography, optical mapping, and a custom mechanical testing system to quantify and relate these parameters. We found a remarkable fine tuning of the AV cushion biomechanics that coincides with a transition in cardiac pumping mechanisms.

Materials and Methods

In Vivo Kinematics

B-Mode, M-Mode, and Doppler blood velocities were recorded from chick atrioventricular (AV) canals at Hamburger and Hamilton[13] (HH) stages 17 through 25 using 55 MHz ultrasound (Vevo660, Visualsonics, Inc; RMV708 scanhead) using a custom built environmental chamber (Figure 1). Images and video frames were transferred to image analysis software (ImageJ, NIH) and filter processed for contrast/edge enhancement. B-Mode, M-Mode, and Doppler-generated contours of tissue motions and blood velocities were traced from 6 to 8 different hearts per stage and aligned in the cardiac cycle according to initial cushion opening (supplemental Figure II, available online at http://circres.ahajournals.org). Myocardial contraction, cushion thickness, and blood velocity parameters were then derived from these data streams and compared using ANOVA with $P<0.05$ denoting significance. Optical recordings of AV canal myocardial activation mapping were obtained as previously described.[14–16] Additional details are provided in the online supplement.

Mesomechanical Testing

Pipette aspiration systems have been developed and used for measuring mechanical properties of cells and tissues that are too small to be tested by conventional techniques.[17] We developed a similar system to measure material properties of embryonic cushions (supplemental Figure III). The superior and inferior AV cushions at different stages of development were isolated from avian hearts at HH17, HH21, and H25, representing early, mid, and late cushion formation stages with myocardial wall intact. Cushions were placed in an isotonic bath supplemented with BSA and other amino acids (RB1 medium, kind gift of S. Kubalak Medical University of South Carolina, Charleston) and positioned to the tip of smoothed tip glass micropipette, and adhered at the central portion of the endocardial surface by a small vacuum pressure not capable of distending the tissue ($P\approx0.1$ Pa). Aspirated tissue length was then measured simultaneously with applied vacuum pressure. Increased pressure resulted in incrementally less aspirated length, suggesting a nonlinear material response. Previous computational and experimental studies by Ohashi et al and Aoki et al investigated the ability of pipette aspiration to measure nonlinear finite elasticity of soft tissues.[17,18] Geometric influences were negligible if the tissue sample was at least 5 times the radius of the pipette in diameter and 4 times the radius of the pipette in thickness, which was the case in all of our tissue samples (supplemental Figure III). They then used strain energy based pseudoelasticity theory to model changes in local tissue mechanics,[18,19] and found that the principal tissue stress was equivalent to the applied pressure. To apply this theory to embryonic cushions, it was therefore assumed that the cushion material response was homogeneous, isotropic, and nonlinear hyperelastic. Billiar and Sacks postulated a pseudoelasticity-based constitutive model for adult valve segments that incorporated an exponential strain energy formulation.[20] As a prerequisite for pseudoelastic theory, cushions were preconditioned with ≈20 loading cycles at low pressure ($0<P<1.0$ Pa) before quasi-static loading to remove previous strain history.[21] 4 to 10 cushions were tested per anatomical position and stage. The nonlinear cushion loading curve (pressure versus stretch ratio) was then modeled using a similar theory as previously described[21] and curve fit by Newton-Gaussian iteration. Material coefficients and effective modulus were compared between cushion location and developmental stage using ANOVA with $P<0.05$ considered significant, and the data were also assessed for curve fitting by Normalized Standard Estimation of the Error (NSE).[22] Additional details are provided in the online supplement.

Structural Constituent Modeling

Avian superior atrioventricular cushions were isolated as previously described from HH21 hearts and enzymatically digested by collagenase 2 (Case; Worthington, 300 U/mL) to remove collagen, hyaluronidase (HAD; Sigma, 100 U/mL) to remove glycosaminoglycans (GAGs), or cytochalasin D (CD; Sigma, 1 μmol/L) to remove cellular traction forces by inhibiting actin polymerization. Each treatment was incubated at 37°C 5% CO_2 for 6 hours under gentle rocking, with untreated cushions serving as controls. 5 to 10 cushions were used per treatment. Mechanical testing was conducted as before, and the resulting modeling curves compared as before. The collagen, cell, and glycosaminoglycan (GAG) specific loading curves were derived from the individual treatment results by appropriating strain energy. Mixture theory was then used to predict material responses based on tissue composition. This assumes the total tissue material response is equivalent to the sum of the individual constituent contributions multiplied by their volume fractions. Serial sections through the AV of 4% paraformaldehyde fixed, paraffin embedded chick embryos from HH17–25 were stained with Movat pentachrome to identify volume fractions of cells, collagen, and glycosaminoglycans using color thresholding. These volume fractions were combined with the derived component material curves using mixture theory to model whole cushion responses, which were compared with the actual loading curves using NSE. Additional details are available in the online supplement.

Results

Transitions in Atrioventricular Function in Vivo

Echocardiography of the embryonic AV canal between HH17 and HH25 shows dramatic changes in cushion motions, indicating important changes in atrioventricular canal mechanics (Figure 1). HH17 cushions were largely acellular as evidenced by histology, a feature which correlated well with the lack of echogenicity in the cardiac jelly (supplemental Movie I). Endocardial and myocardial contours traced from these frames show the early cushions had an almost unmeasurable thickness by ultrasonography during the open filling phase (Figure 2, top), but increased in thickness to coapt during peak contraction of the AV myocardium (130 μm thick, 30% contraction at approximately 0.8 cycle fraction). The cushions then "treadmilled" longitudinally down the AV canal. Once the longitudinal tissue contraction wave reached the ventricular segment, the canal opened, the cushions retracted, and blood flow was reinitiated. The cushions exhibited simultaneous changes in thickness with the myocardium through the cardiac cycle at the limits of M-mode resolution. HH17 AV blood flow was biphasic: the first phase coincided with canal opening and carried the majority of the flow energy (Figure 3), whereas the second phase correlated with the acceleration in myocardial contraction preceding cushion coaptation. Maximum blood velocity measured in each phase was approximately 3.0 cm/s.

HH21 endocardial and myocardial AV contours (Figure 2, middle panels and supplemental Movie II) showed persistent thickness throughout the cardiac cycle, ranging from 140 to 260 μm, rather than longitudinal treadmilling. The cushions rocked caudally such that their coaptation occurred at a point (or line in 3D) that translated along the AV canal. Also unlike HH17, changes in tissue thickness were approximately 0.20

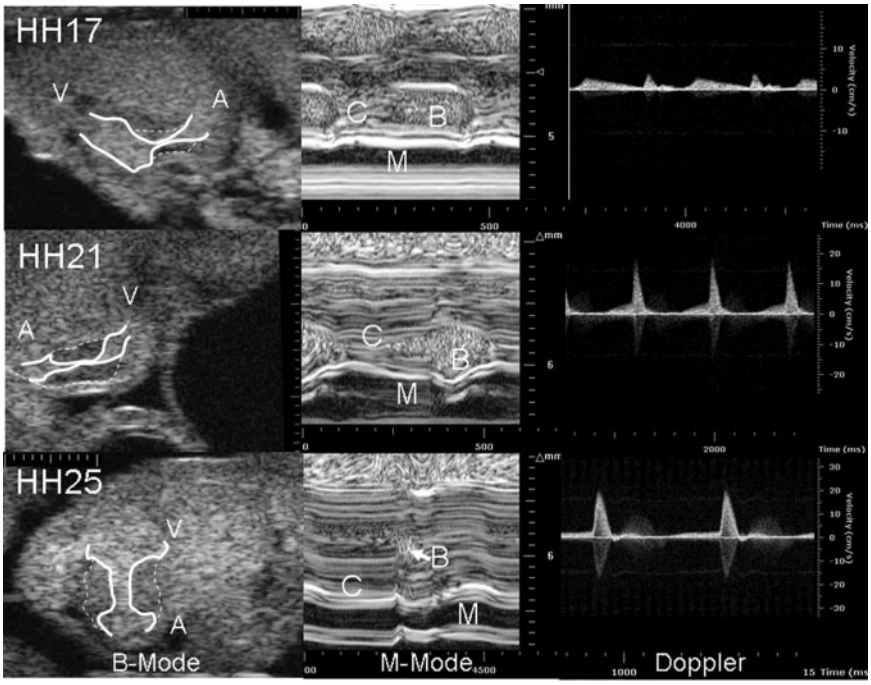

Figure 1. 55-MHz transducer ultrasound videos and images of HH17, HH21, and HH25 chick atrioventricular canals. Left panels indicate B-Mode videos of AV long-axis from which cushion (solid) and myocardial (dashed) motions were traced. Middle panels show transverse axis M-Mode images of the AV crossection, from which time course information of cushion (A), blood (B), and myocardium (C) is gathered. Right panels show Doppler ultrasound of blood velocity through the AV canal at each stage. Scale marks=100 μm.

cycle (72 degrees) out of phase with the contraction of the myocardium. Peak cushion thickness occurred within the range of peak AV myocardial contraction (again 30%), but minimum thickness occurred while the myocardium is rapidly contracting. Blood flow at this stage was also markedly different. Though still biphasic, the initial phase had much slower blood velocity than the second, which now carried most of the flow energy. AV canal flow pathways were still mostly open during the cardiac cycle (Figure 3).

At HH25, as can be seen in Figure 2, bottom panels (and supplemental Movie III), there was no longer any longitudinal tissue motion through the AV canal and the cushions coapted along their entire length simultaneously. The cushions came together and parted rapidly, and the principle flow was a single atrially propelled jet of blood. Cushion thickness varied in phase with the myocardial contraction, becoming thinnest (260 μm) at peak myocardial relaxation and thickest (450 μm) at peak contraction (now only 16%). Average peak blood velocity during this phase was 17.1 cm/s (Figure 3). Our reported AV Doppler velocity profiles compare well with previously published studies.[23,24]

Comparison of tissue motions and blood flow from each stage suggested that the flow regulation mechanics of the AV canal were tied directly to the material properties of the cushions (Figure 4). A significant inverse linear correlation is apparent when comparing the tissue wave speed and peak blood velocity between embryos over stages 17 to 25 (R=0.899). The nearly acellular gelatinous AV cushions of HH17 heart undulated as a wave with myocardial contraction. The tissue wave speed was approximately 8 mm/s, slower than the peak blood flow. Myocardial tissue wave velocity was diminished at HH21 (≈6 mm/s), whereas peak blood flow velocity was increased (≈11 cm/s). There was persistent though changing thickness of the cushions throughout the cardiac cycle during compression and stretching. At HH25, there was almost no tissue wave (≈2 mm/s) yet the peak blood velocity was much higher (≈20 cm/s). The cushions at this stage change less in thickness over the cardiac cycle than the other stages, suggesting that they were more rigid. These findings highlight changes of AV canal cushion mechanics as being critical to the normal function of the AV canal in regulating unidirectional blood flow.

Alterations in Atrioventricular Conduction Patterns

The propagation of the myocardial depolarization signal changes significantly between HH17 and HH25. As shown in Figure 5, depolarization at HH17 was activated at the superior aspect of the primitive atrial segment (*) and progressed in a pseudo-linear manner as indicated by the isochrone lines through the ventricular and outflow segments, compatible with peristaltic/suction pumping. At HH21 the conduction pattern began to transition to a binodal configuration. Depolarization progressed radially through the atrium to the atrioventricular canal, followed by earliest ventricular activation of a portion of the superior ventricle near the inner curvature. By HH25, depolarization of the atria was followed by ventricular activation that was earliest at a zone clearly distant from the AV canal and which then spread independently through the right and left ventricular myocardial tissues (*), supporting function as independent piston-like pumps. To determine the velocity of conduction propagation through the atrioventricular canal at these different stages, the length of the canal was measured using the B-Mode ultrasound images, this length being between the initial and final cushion extremes. This length was then divided by the conduction delay (approximately 49, 40, and 46 ms, respectively), which resulted in HH17, HH21, HH25 conduction velocities being 20.1, 18.4, and 10.3 mm/s,. respectively. These results show that AV conduction velocity is slowing concomitant with the mesenchymal growth of the cushions, as has been previously shown.[25]

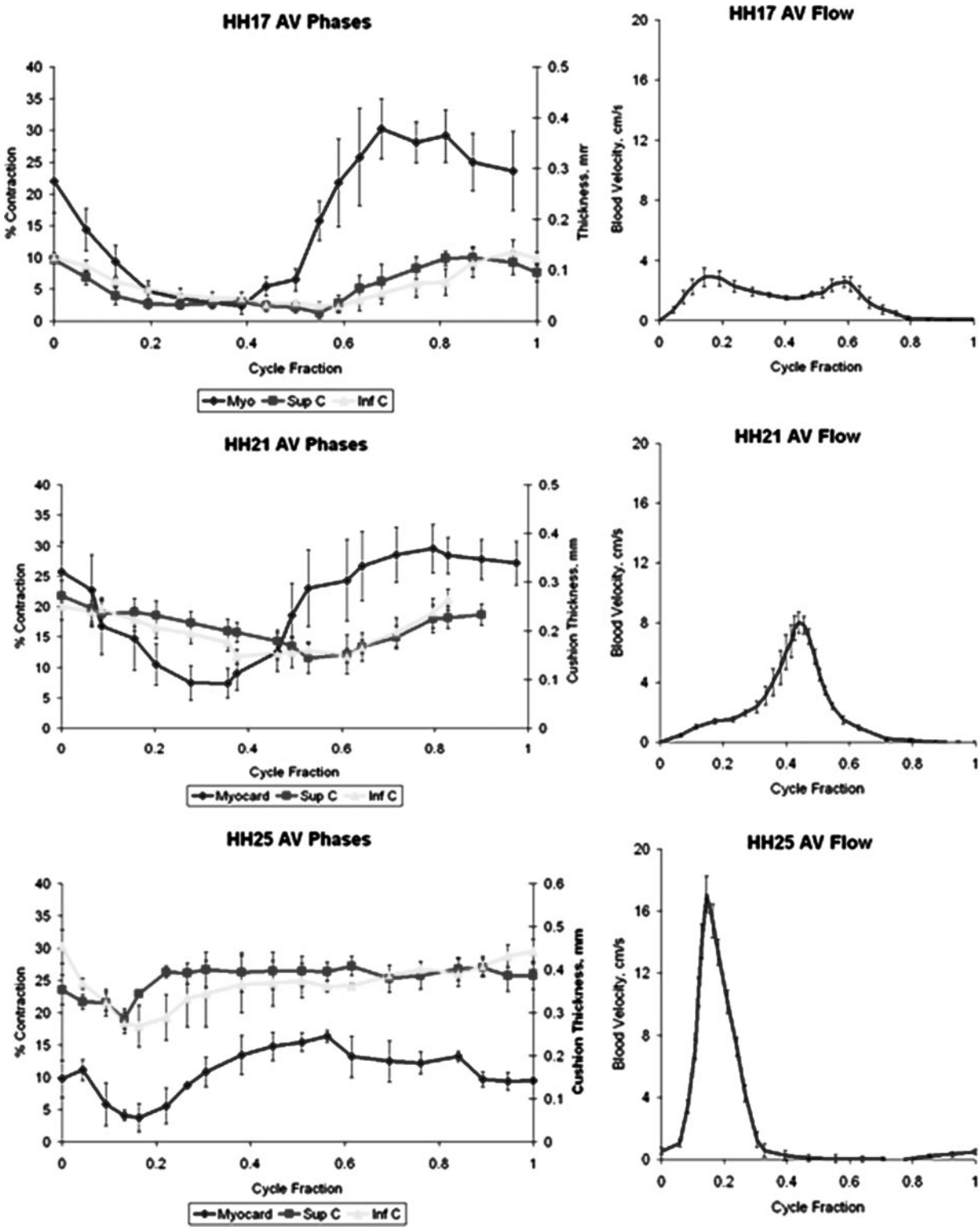

Figure 2. Comparison of M-Mode (left) and Doppler (right) data from HH17 (top), HH21 (Middle) and HH25 (bottom) AV canals. Data was generated from 6 M-Modes and 6 Dopplers of the same hearts. Curves denote average readings and error bars indicate SEM.

Nonlinear Pseudoelastic Material Modeling of Developing AV Valve Cushions

To quantify changes in AV cushion material properties during these stages, a mesomechanical test system was developed to apply tensile tests to these small tissues while limiting gripping artifacts. The stress-strain loading curves of isolated valve cushions all showed a monotonically increasing nonlinear mechanical response. As evidenced by low NSE values, our data were modeled well by pseudoelasticity theory, but there were distinct differences between developmental stage (Figure 6 and supplemental Table I). Generally, both AV cushions were extremely pliable at HH17 ($E_{Eff} \approx 0.15$

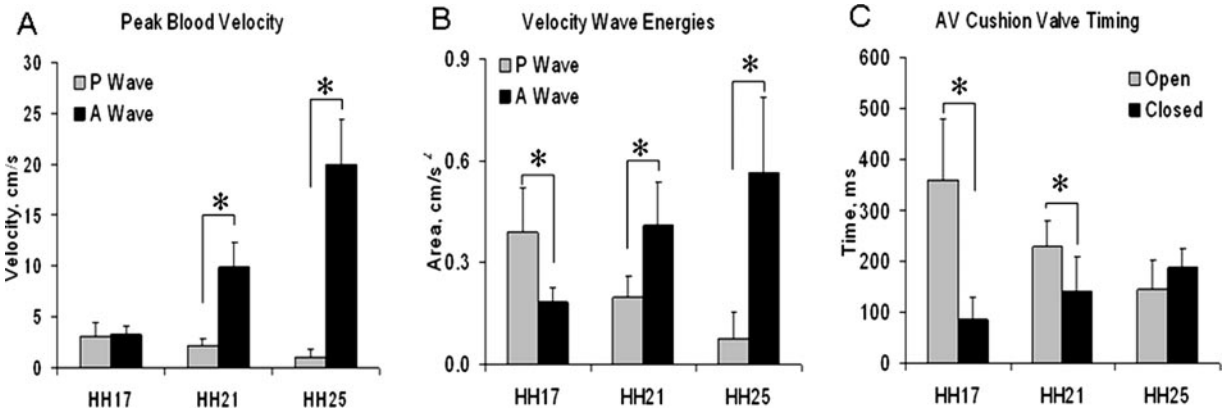

Figure 3. Characterization of atrioventricular hemodynamics by Doppler ultrasound. Velocity waves were parsed into primary "passive" and secondary "active" components from at 6 to 10 samples per condition. A, Peak blood velocities at each stage. B, Wave energies as determined by the area under the velocity/time curve. C, AV Valve timing as determined by M-Mode data.

Pa) but became successively more rigid at HH21 (E_{Eff}≈0.85 Pa) and HH25 (E_{Eff}≈3.6 Pa). Effective moduli were statistically significant between stages ($P<0.05$), but not between cushions. Statistical differences between linear and nonlinear coefficients (supplemental Table I) suggested that the mechanical response of HH17 inferior and superior AV cushions were different, but similar at HH21 and HH25.

Composite Modeling Predicts Cushion Material Properties

Specific enzymatic digestion treatments were applied to HH21 AV cushions to ascertain the contribution of collagen, GAGs, and cells to the material properties. As shown in Figure 7A and 7B, hyaluronidase digestion resulted in a very nonlinear rigid cushion, whereas collagenase digestion resulted in an extremely fragile, more linear elastic tissue. Cytochalasin D treatment of cushions resulted in minimal differences compared with control tissues, and only at large stretch ratios (also supplemental Table I) and without significant differences in effective modulus, suggesting that cell traction forces are not significant contributors to the material properties of the AV cushions at these stages of development.

Histological staining of AV valve cushions at HH17 through HH25 shows dramatic changes in cushion morphology and composition (supplemental Figure IV). It is important to note that from a biomechanical perspective, the structural composition of the material is the driving factor in the material properties of the tissue rather than the size of the tissue or absolute amounts of the constituents. HH17 AV cushions are comprised mostly of GAGs (hyaluronan), but some invading cells are present. Between HH21 and HH25, AV cushions increase in collagen and cell proportion, and image analysis shows that collagen and cell content approach 30% each of the total cushion volume (Figure 8A and 8B).

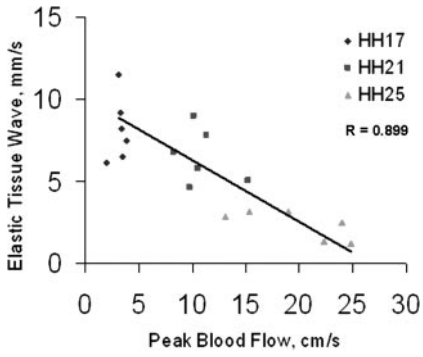

Figure 4. A strong correlation exists between peak blood flow and tissue wave propagation in AV canals of different stage embryos. The left side of the graph contains hearts in a suction-pumping condition, whereas the right side approaches piston-pumping. The ratio of velocities highlights a near-linear transition between these two functional states.

Interestingly, the derived individual component loading curves (Figure 7C) were similar in trend to the stage specific cushion loading curves, suggesting that cushion structure may regulate tissue biomechanics. To this end, composite modeling of the cushions at HH17 and HH25 was achieved by combining the component strain energies for GAGs, collagen, and cell traction fractions determined from HH21 cushions with the HH17 and HH25 histologically determined volume fractions. Because CD treatments resulted in little differences in material response and cushion mesenchymal cells were surrounded by collagen fibers at HH21 and HH25, we postulated that the collagen volume fractions at these stages were better represented mechanically by adding to it the cell volume fraction. The component fractions are shown in supplemental Table II, and the resulting curves are shown in Figure 8C and 8D. The mixture model generally predicted the measured material response to tensile stress at HH17 and HH25 for both superior and inferior cushions. The low NSE values for these curves indicate that these curves are still relatively accurate given the number of data points and small number of empirical coefficients. These results show that good prediction of the mechanical properties of valvular cushions were possible by composite modeling of the component volume fractions.

Discussion

Embryonic heart development is characterized by dramatic growth and change over a relatively short amount of time, all the while generating unidirectional blood flow. Prior models of endocardial cushion function and their contribution to flow regulation have not accounted for cushion material properties and have been biomechanically oversimplified. The results of

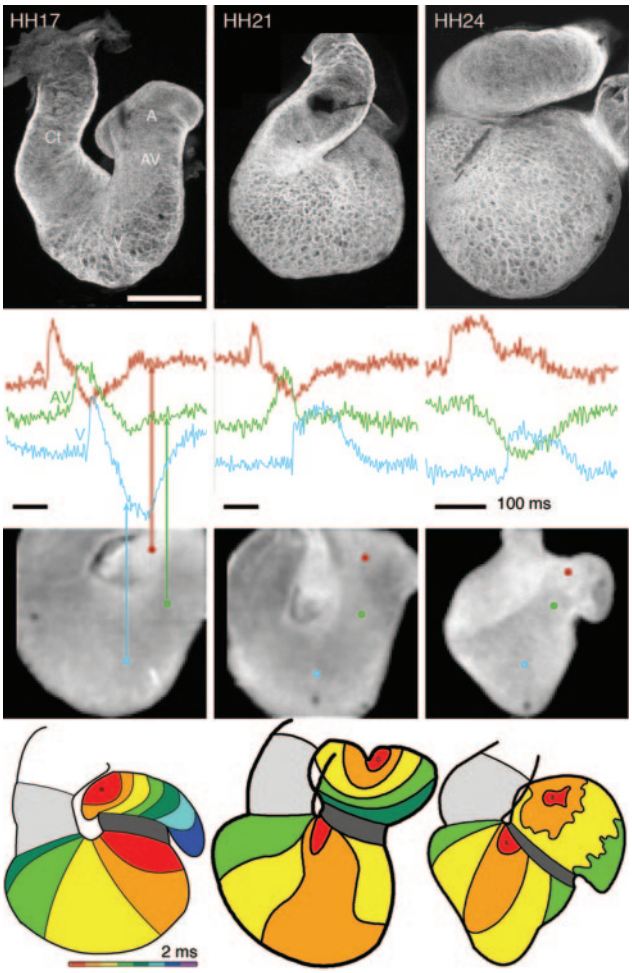

Figure 5. Developmental changes in heart activation. Top row, Maximum intensity projection confocal images from rhodamine-phalloidin stained hearts (method by Germroth et al). Scale bar 500 μm. Second row, Optically recorded action potentials from different heart compartments (raw data). The atrioventricular delay in these examples is 122, 131, and 115 ms, respectively. Time scale 100 ms. Note that the upstroke velocity is slower at the AV region, and at the latest studied stage it is impossible to obtain signal from it (only contraction-related motion is present). Below are shown actual images (80×80 pixels) from the CCD camera. Activation maps in the bottom show separately the atrial and ventricular isochrones in 2 ms intervals. Dark stippling denotes the AV region, light gray marks the contractile part of the conotruncus.

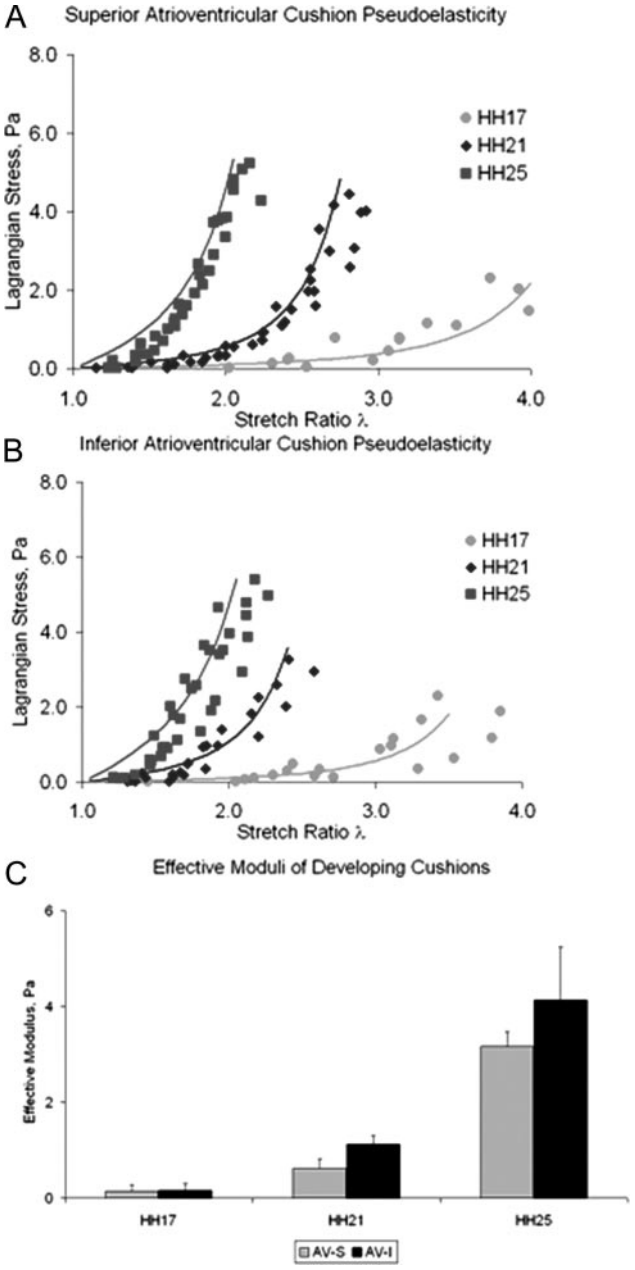

Figure 6. Pseudoelastic modeling of embryonic cushions. Superior (A) and Inferior (B) cushions were tested using the mesomechanical aspiration device, and the resulting data were modeledusing pseudoelasticity theory (solid line). The averaged α and C values for an entire data set (4 to 7 cushions) was used to determine the goodness of fit of the data (shown in supplemental Table I). C, Effective moduli of cushions according to $M=\alpha C$. Each stage is significantly different ($P<0.05$) from the others, but no differences were observed between anatomical position.

the current study link hemodynamic function with myocardial activation and cushion mechanics to show the spectrum of atrioventricular flow regulation during the transition from a single AV lumen to separate right and left atrioventricular connections. Our studies show a defined progression in AV canal mechanics necessary for the transition in cardiac function from a suction-like pump at HH17 to a piston-like pump at HH25. The relatively weak HH17 cushions are propelled in a treadmill-like fashion by the contracting myocardium, which occurs in a quasi-linear fashion along the looped heart tube. During migration, mesenchymal cells secrete collagen (HH21), rendering the cushions more rigid and assuming rocking mechanics, rather than a wave-like mechanism of apposition. Slowing of AV myocardial conduction and increases in AV blood flow velocities are also noted. By HH25, the cushion mechanics resembled rigid structures meeting along a broad zone of apposition—a probable prelude to successful AV cushion fusion. When fully populated with mesenchyme, cushions contained much more collagen, and exhibited increases in thickness and rigidity. The AV myocardial conduction velocity was further decreased, whereas the AV blood flow velocity was further increased. The increases of blood flow velocity observed, and the transition from passive early filling dominance to atrial

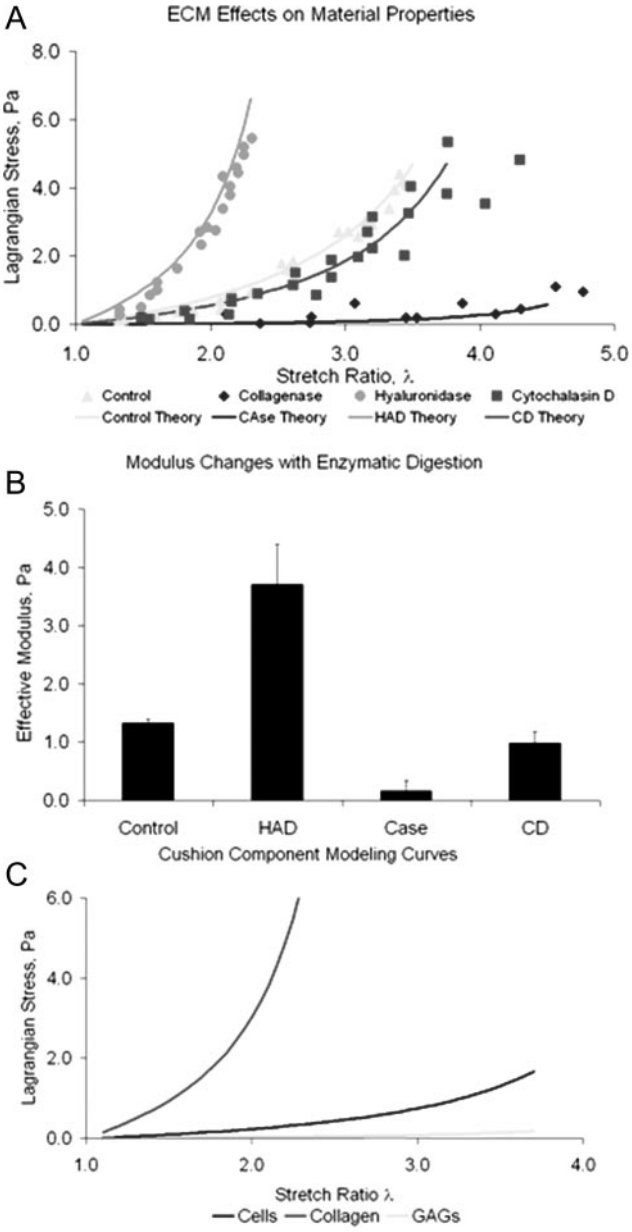

Figure 7. The effects of enzymatic and biochemical treatments of HH21 superior AV cushions on material properties. Cushions were treated for 6 hours with either hyaluronidase (HAD), collagenase (Case), or cytochalasin D (CD), followed by mechanical testing. The stress-strain curves are shown in A, and effective modulus in B. Significant differences were recorded in all cases except control vs CD ($P<0.05$). 5 to 10 cushions were used in each condition. By partitioning the strain energy of the reactions, the stress–strain response of the individual components could be approximated (C).

contraction dominance, correspond to the atrioventricular canal flow channels becoming more restrictive in relation to the net volume of blood crossing the AV junction as the junction remodels.

A seminal study by Foruohar et al determined that the early zebrafish heart functions as a suction pump through the several criteria, most notably that (1) maximum cushion thickness occurs at peak myocardial contraction, (2) blood velocity exceeds that of tissue velocity, and (3) wave propagation is initiated by a single myocardial source.[5] Our HH17 data are consistent with these criteria, suggesting that this stage chick heart may also behave like a suction pump, in contrast to the peristaltic mechanism previously suggested. A thermodynamic characterization of piston pumping is a volume change–driven propulsion of fluid, with negligible contribution to pumping by the orifice except to throttle the outlet flow. Our data at HH25 is again consistent with this notion, and therefore appears that the HH21 AV may be a transitional stage between 2 pumping styles.

Our data show that material properties of embryonic prevalvular tissues change in concert with changes in their observed mechanics. Using the enzymatic digestions and Cytochalasin D treatments, the individual contributions of collagen, GAGs, and cell traction forces were approximated. Collagen contributed to the majority of the cushion tissue nonlinear rigidity, as has been shown for numerous soft tissues. GAG (mostly hyaluronan in these tissues) material properties were found to be extremely weak, extensible, and mostly linear. Previous studies measuring the material properties of cartilage, which also contains glycosaminoglycans, showed that hydration and swelling also contribute to biomechanical response.[26] GAGs are complex, highly coiled chains that exhibit entropic elasticity: they resist uncoiling from stretching to maintain disorder. The mechanical contribution of GAGs in valve cushions is likely attributable to a combination of entropic elasticity and altered extracellular matrix hydration properties.

We used mixture theory to combine the stress-strain behavior attributable to individual components and found that material properties could be reasonably predicted across developmental stage and anatomical position. Similar formulations were applied to predict material behavior in the aorta as a function of collagen, elastin, and cell contractions, and could predict functional consequences of alterations in component configurations.[22] Deviations in the model at large strains of HH25 AV cushions may be caused by unmodeled interaction effects between constituents or from additional cell/matrix components not considered. This is most clearly demonstrated by the apparent negative strain energy induced by HAD treatment in Figure 7C, resulting in a more rigid tissue but thermodynamically impossible. We believe that the HAD effect is the result of the removal of an important but as yet unknown interaction effect between GAGs and collagen. Indeed, it is likely that all of the assumptions posed in this model will need to be revisited in more complex experimental and computational models,[20] but nevertheless these results demonstrate the utility of this simplified model for predicting material response to changes in matrix.

Hemodynamics may be an important factor in cushion tissue strengthening required for embryonic development to progress. Temporal increases in blood pressure and blood flow velocity must be supported by changes in cushion tissue structure to ensure proper structural integrity. The increasing cushion tissue elastic rigidity with developmental stage reported here may help to maintain morphological integrity under increasing mechanical stress, as has been postulated in adult valves.[27] The nonlinear nature of the stress-strain curve suggests the tissue is pliable under lighter loads but has an innate resistance to deformation by increased loads. This

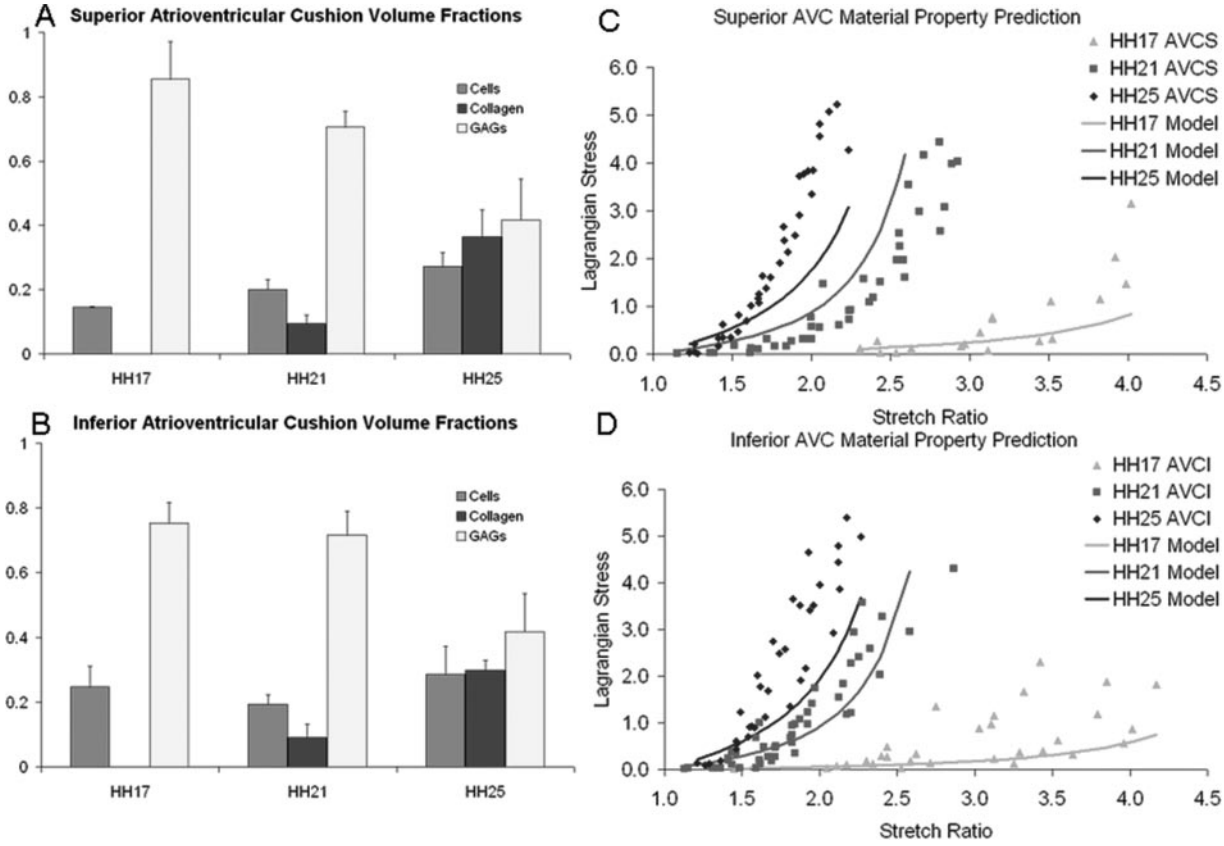

Figure 8. Cushion structural composition predicts material properties. The volume fractions of cells, collagen, and GAGs for the superior and inferior AV cushions are shown in A and B, respectively. These were combined with the individual component modeling curves via mixture theory to predict material properties for the other stages and positions, which are shown in C and D. Solid lines indicate theoretical curves, and individual points represent the data. Good correlations as evidenced by low NSE values at all stages and conditions were realized. Underestimation of material properties were apparent at large stretch ratios at HH25, suggesting the presence of components or component interactions at that stage not encompassed in our model.

suggests that cushions can preserve their structure under a wide range of hemodynamic forces, and in that way inhibit regurgitation under temporary variations from ideal hemodynamic conditions.

Appropriate transitions in AV cushion properties are likely to include signaling through the endocardial cells that line the lumenal surface of the cushions. It is already known that these cells are unique in their ability to undergo EMT, but they may also play a role in regulating post-EMT cushion morphogenesis through integration of hemodynamic stimuli and signaling of underlying mesenchyme. Vascular endothelial cells are the primary mechanosensitive agents in normal vascular function. Germane to this discussion, it was recently shown that adult valvular endothelial cells possess mechanosensitive functions not shared by vascular endothelial cells,[28] and can stimulate valvular interstitial cells in coculture in response to shear stress.[29] This raises the question whether similar mechanosensitivity mechanisms are factors in normal and abnormal cushion and valvular development. Several studies have shown that obstructing or altering blood flow patterns results in defective heart development.[1,30,31] One recent study demonstrated changes in embryonic endocardial expression of mechanosensitive genes in vivo by altered hemodynamic loading.[32] These and the results of this study point to endocardial cells as excellent candidates for the mechanosensitive signaling in normal morphological and physiologic cushion morphogenesis.

How endothelial signaling corresponds with myocardial contractile function is currently unknown, but many of the signals implicated in EMT, such as bone morphogenetic proteins, transforming growth factor beta, and vascular endothelial growth factor, require coordination between the myocardium and endocardium.[7,33–35] The role of hemodynamics in EMT is still controversial. One study suggests that disruption of myocardial contraction (and likely flow) is sufficient to inhibit EMT.[36] The fact that EMT can be initiated in vitro through the expression or inhibition of a variety of signals (reviewed by Person et al[37]) without hemodynamics does not rule out a necessary role for hemodynamic processes in vivo.

Our article therefore adds to the conclusion that biomechanics play an important signaling role in valvulogenesis. There are many examples where genetic deficiencies result in altered biomechanical properties, which over time lead to early valvular degeneration, as in some palliated congenital heart defects[38] as well as functional defects like bicuspid aortic valve, myxomatous valves, and mitral valves in patients with Marfan syndrome. It may be that biomechanical abnormalities arising from a number of genetic causes may contribute to the development of abnormal morphological phenotypes such as common AV canal as well as normal

structures that subsequently become dysfunctional prematurely. New biomechanical tools and analytical techniques such as those presented in this study will help to characterize more subtle phenotypes with greater predictive power and, ultimately, clinical potential.

Sources of Funding

This work was funded in part by an NIH training grant in pediatric cardiology (HL007710 to J.T.B.), RR16434 (to R.R.M., T.C.M.), HL/HD67135 (to T.C.M.), VZ 206100-3 from the Ministry of Education of the Czech Republic, IRP IAPG AVOZ50450515 from the Academy of Sciences of the Czech Republic, and Purkinje Fellowship from the Academy of Sciences of the Czech Republic (to D.S.). J.T.B., T.C.M., D.T., and R.R.M. conducted their work in a facility constructed with support from the National Institutes of Health, Grant Number C06 RR018823 from the Extramural Research Facilities Program of the National Center for Research Resources.

Disclosures

None.

References

1. Sedmera D, Pexieder T, Rychterova V, Hu N, Clark EB. Remodeling of chick embryonic ventricular myoarchitecture under experimentally changed loading conditions. *Anat Rec*. 1999;254:238–252.
2. Ishiwata T, Nakazawa M, Pu WT, Tevosian SG, Izumo S. Developmental changes in ventricular diastolic function correlate with changes in ventricular myoarchitecture in normal mouse embryos. *Circ Res*. 2003;93:857–865.
3. Keller BB, MacLennan MJ, Tinney JP, Yoshigi M. In vivo assessment of embryonic cardiovascular dimensions and function in day-10.5 to -14.5 mouse embryos. *Circ Res*. 1996;79:247–255.
4. Patten B, Kramer T, Barry A. Valvular action in the embryonic chick heart by localized apposition of endocardial masses. *Anat Rec*. 1948;102:299–311.
5. Forouhar AS, Liebling M, Hickerson A, Nasiraei-Moghaddam A, Tsai HJ, Hove JR, Fraser SE, Dickinson ME, Gharib M. The embryonic vertebrate heart tube is a dynamic suction pump. *Science*. 2006;312:751–753.
6. Jackson LF, Qiu TH, Sunnarborg SW, Chang A, Zhang C, Patterson C, Lee DC. Defective valvulogenesis in HB-EGF and TACE-null mice is associated with aberrant BMP signaling. *Embo J*. 2003;22:2704–2716.
7. Chang CP, Neilson JR, Bayle JH, Gestwicki JE, Kuo A, Stankunas K, Graef IA, Crabtree GR. A field of myocardial-endocardial NFAT signaling underlies heart valve morphogenesis. *Cell*. 2004;118:649–663.
8. Alford PW, Taber LA. Regional epicardial strain in the embryonic chick heart during the early looping stages. *J Biomech*. 2003;36:1135–1141.
9. Taber LA, Perucchio R. Stress-strain relations in embryonic chick heart. *Am J Physiol Heart Circ Physiol*. 2001;281:H463–H466.
10. Billiar KL, Sacks MS. Biaxial mechanical properties of the natural and glutaraldehyde treated aortic valve cusp–Part I: Experimental results. *J Biomech Eng*. 2000;122:23–30.
11. Grashow JS, Yoganathan AP, Sacks MS. Biaixal stress-stretch behavior of the mitral valve anterior leaflet at physiologic strain rates. *Ann Biomed Eng*. 2006:1–11.
12. Leeson-Dietrich J, Boughner D, Vesely I. Porcine pulmonary and aortic valves: a comparison of their tensile viscoelastic properties at physiological strain rates. *J Heart Valve Dis*. 1995;4:88–94.
13. Hamburger V, Hamilton HL. A series of normal stages in the development of the chick embryo. 1951. *Dev Dyn*. 1992;195:231–272.
14. Reckova M, Rosengarten C, deAlmeida A, Stanley CP, Wessels A, Gourdie RG, Thompson RP, Sedmera D. Hemodynamics is a key epigenetic factor in development of the cardiac conduction system. *Circ Res*. 2003;93:77–85.
15. Sedmera D, Reckova M, Bigelow MR, Dealmeida A, Stanley CP, Mikawa T, Gourdie RG, Thompson RP. Developmental transitions in electrical activation patterns in chick embryonic heart. *Anat Rec A Discov Mol Cell Evol Biol*. 2004;280:1001–1009.
16. Sedmera D, Wessels A, Trusk TC, Thompson RP, Hewett KW, Gourdie RG. Changes in activation sequence of embryonic chick atria correlate with developing myocardial architecture. *Am J Physiol Heart Circ Physiol*. 2006;291:H1646–H1652.
17. Aoki T, Ohashi T, Matsumoto T, Sato M. The pipette aspiration applied to the local stiffness measurement of soft tissues. *Ann Biomed Eng*. 1997;25:581–587.
18. Ohashi T, Abe H, Matsumoto T, Sato M. Pipette aspiration technique for the measurement of nonlinear and anisotropic mechanical properties of blood vessel walls under biaxial stretch. *J Biomech*. 2005;38:2248–2256.
19. Matsumoto T, Abe H, Ohashi T, Kato Y, Sato M. Local elastic modulus of atherosclerotic lesions of rabbit thoracic aortas measured by pipette aspiration method. *Physiol Meas*. 2002;23:635–648.
20. Billiar KL, Sacks MS. Biaxial mechanical properties of the native and glutaraldehyde-treated aortic valve cusp: Part II–A structural constitutive model. *J Biomech Eng*. 2000;122:327–335.
21. Fung Y. *Biomechanics: Mechanical Properties of Living Tissues.* Second ed. New York: Springer-Verlag; 1993.
22. Armentano RL, Barra JG, Levenson J, Simon A, Pichel RH. Arterial wall mechanics in conscious dogs. Assessment of viscous, inertial, and elastic moduli to characterize aortic wall behavior. *Circ Res*. 1995;76:468–478.
23. Hu N, Clark EB. Hemodynamics of the stage 12 to stage 29 chick embryo. *Circ Res*. 1989;65:1665–1670.
24. Campbell KA, Hu N, Clark EB, Keller BB. Analysis of dynamic atrial dimension and function during early cardiac development in the chick embryo. *Pediatr Res*. 1992;32:333–337.
25. de Jong F, Opthof T, Wilde AA, Janse MJ, Charles R, Lamers WH, Moorman AF. Persisting zones of slow impulse conduction in developing chicken hearts. *Circ Res*. 1992;71:240–250.
26. Best BA, Guilak F, Setton LA, Zhu W, Saed-Nejad F, Ratcliffe A, Weidenbaum M, Mow VC. Compressive mechanical properties of the human anulus fibrosus and their relationship to biochemical composition. *Spine*. 1994;19:212–221.
27. Robicsek F, Thubrikar MJ, Cook JW, Fowler B. The congenitally bicuspid aortic valve: how does it function? Why does it fail? *Ann Thorac Surg*. 2004;77:177–185.
28. Butcher JT, Tressel S, Johnson T, Turner D, Sorescu G, Jo H, Nerem RM. Transcriptional profiles of valvular and vascular endothelial cells reveal phenotypic differences: influence of shear stress. *Arterioscler Thromb Vasc Biol*. 2006;26:69–77.
29. Butcher JT, Nerem RM. Valvular endothelial cells regulate the phenotype of interstitial cells in co-culture: effects of steady shear stress. *Tissue Eng*. 2006;12:905–915.
30. Hogers B, DeRuiter MC, Gittenberger-de Groot AC, Poelmann RE. Extraembryonic venous obstructions lead to cardiovascular malformations and can be embryolethal. *Cardiovasc Res*. 1999;41:87–99.
31. Hove JR, Koster RW, Forouhar AS, Acevedo-Bolton G, Fraser SE, Gharib M. Intracardiac fluid forces are an essential epigenetic factor for embryonic cardiogenesis. *Nature*. 2003;421:172–177.
32. Groenendijk BC, Hierck BP, Vrolijk J, Baiker M, Pourquie MJ, Gittenberger-de Groot AC, Poelmann RE. Changes in shear stress-related gene expression after experimentally altered venous return in the chicken embryo. *Circ Res*. 2005;96:1291–1298.
33. Ma L, Lu MF, Schwartz RJ, Martin JF. Bmp2 is essential for cardiac cushion epithelial-mesenchymal transition and myocardial patterning. *Development*. 2005;132:5601–5611.
34. Yamagishi T, Nakajima Y, Miyazono K, Nakamura H. Bone morphogenetic protein-2 acts synergistically with transforming growth factor-beta3 during endothelial-mesenchymal transformation in the developing chick heart. *J Cell Physiol*. 1999;180:35–45.
35. Sugi Y, Yamamura H, Okagawa H, Markwald RR. Bone morphogenetic protein-2 can mediate myocardial regulation of atrioventricular cushion mesenchymal cell formation in mice. *Dev Biol*. 2004;269:505–518.
36. Bartman T, Walsh EC, Wen KK, McKane M, Ren J, Alexander J, Rubenstein PA, Stainier DY. Early myocardial function affects endocardial cushion development in zebrafish. *PLoS Biol*. 2004;2:E129.
37. Person AD, Klewer SE, Runyan RB. Cell biology of cardiac cushion development. *Int Rev Cytol*. 2005;243:287–335.
38. Glen S, Burns J, Bloomfield P. Prevalence and development of additional cardiac abnormalities in 1448 patients with congenital ventricular septal defects. *Heart*. 2004;90:1321–1325.